大規模詳細反応機構を考慮可能な高効率流体解析手法

An efficient methodology for combustion flow simulations with large detailed chemical kinetic mechanisms

○寺島　洋史（北海道大学）

社会連携講座　反応性熱流動研究グループ

2013年4月 - 2015年11月　社会連携講座　特任准教授

Backgrounds

- Understanding combustion flow fields of liquid rocket engines

- CFD (Fluid dynamics) simulations
- Detailed chemical kinetics

‣ Combustion-related problems in developments

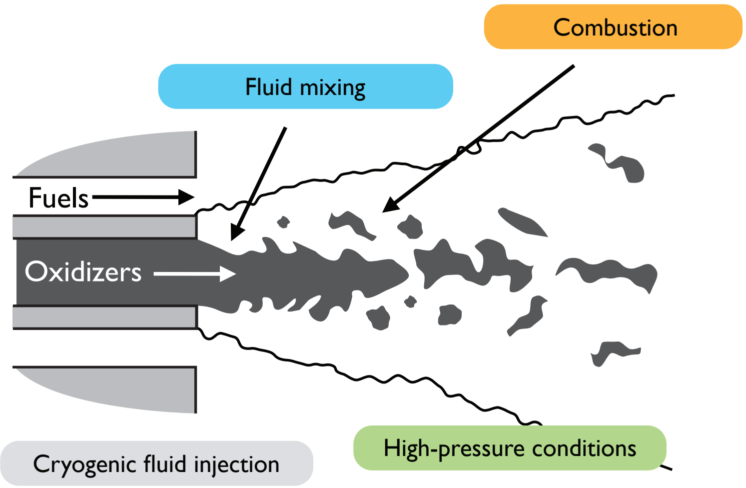

SSME injector damage

Schematic for flow fields of a coaxial jet in liquid rocket engines

Issues on CFD with detailed chemistry

- The Navier-Stokes equations
- Species-mass conservation equations

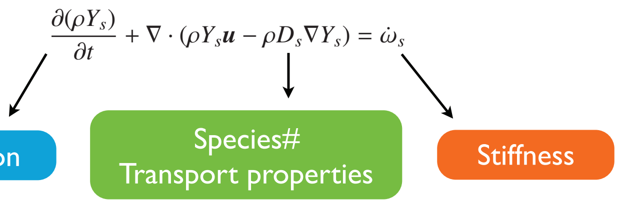

$$\frac{\partial(\rho Y_s)}{\partial t} + \nabla\cdot(\rho Y_s \boldsymbol{u} - \rho D_s \nabla Y_s) = \dot{\omega}_s$$

Spatial resolution

Species#
Transport properties

Stiffness

1) Stiffness in the chemical reaction equations

- A lot of species : Δt=O(1)~O(-15) -- wide range of timescale
  - Time step size is usually determined by the fastest timescale
- This issue is the case even with small reaction mechanisms

$$\frac{\mathrm{d}Y_s}{\mathrm{d}t} = \frac{\dot{\omega}_s}{\rho}, \quad \text{ODE}$$
$$\frac{\mathrm{d}T}{\mathrm{d}t} = -\frac{\sum_{s=1}^{N} e_s \dot{\omega}_s}{\rho c_v},$$

2) The number of chemical species

- The number of species to be advected; the cost proportional to the order of O(N)
- The cost for calculating the transport properties for mixture with the order of O(N^2) required in conventional mixture models

$$\sum_i^N \sum_j^N \phi_{ij}$$

3) Spatial resolution

- The grid requirement may be severe due to the interaction between chemical species and fluids

Computational costs of various terms

- Estimated from computational results of a combustion problem with n-C_4H_{10}, 113 species

VODE

- a standard implicit ODE solver usually used for detailed chemistry

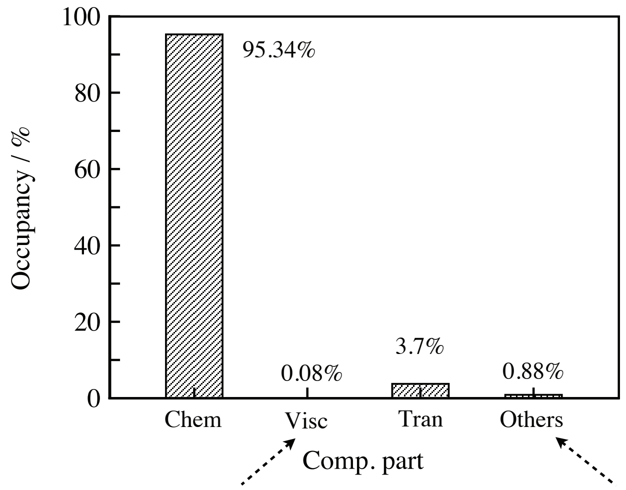

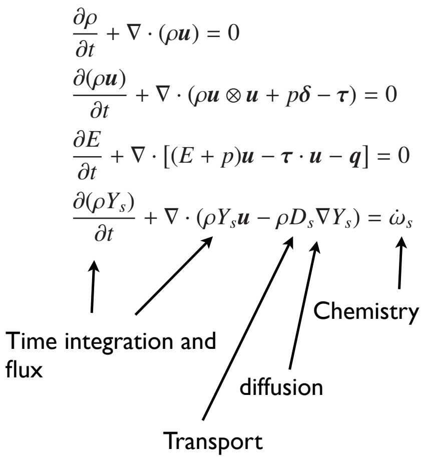

$$\frac{\partial\rho}{\partial t} + \nabla\cdot(\rho\boldsymbol{u}) = 0$$
$$\frac{\partial(\rho\boldsymbol{u})}{\partial t} + \nabla\cdot(\rho\boldsymbol{u}\otimes\boldsymbol{u} + p\boldsymbol{\delta} - \boldsymbol{\tau}) = 0$$
$$\frac{\partial E}{\partial t} + \nabla\cdot[(E+p)\boldsymbol{u} - \boldsymbol{\tau}\cdot\boldsymbol{u} - \boldsymbol{q}] = 0$$
$$\frac{\partial(\rho Y_s)}{\partial t} + \nabla\cdot(\rho Y_s\boldsymbol{u} - \rho D_s\nabla Y_s) = \dot{\omega}_s$$

viscous, heat, and diffusion terms

flux, time integration for fluids and exchange part

Occupancy of CPU times of each computational part

Explicit methods for stiff ODE

- Runge-Kutta method
  (Kennedy and Carpenter, 2003)
- CHEMEQ2
  (Mott et al., 2000, Quresh and Prosser, 2007)
  - Predictor-corrector method based on quasi-steady-state assumption (QSS)
  - Numerical instability

robustness

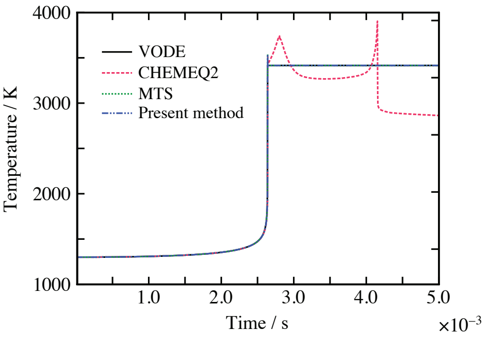

0-D ignition problem for CH_4/O_2, 1 atm, 1300 K

- MTS method
  (Gou et al., 2010, Terashima et al., 2014)

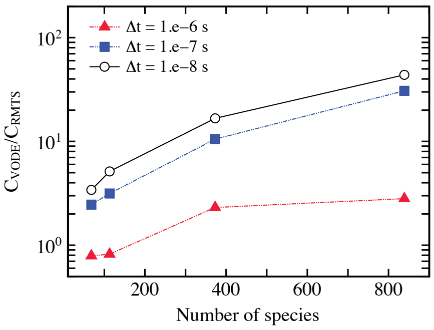

- Chemical species grouped and integrated based on their characteristic times
- Start-up cost for generating groups of chemical species required at each step: faster performance limited with O(1-2)

faster with O(2-3)

Speed-up factor by MTS compared to VODE

ERENA: fast and robust explicit integration method

*Extended Robust Explicit Numerical Algorithm (ERENA)

Y. Morii, H. Terashima, M. Koshi, T. Shimizu, and E. Shima, *Journal of Computational Physics*, 2016.

Governing equations

$$\boxed{\frac{dY_s}{dt} = \frac{\dot{\omega}_s}{\rho} = q_s - p_s Y_s}$$

where $p_s = \frac{c_s}{\rho}, \quad q_s = \frac{d_s}{\rho Y_s}$

c_s : creation rate of species
d_s : destruction rate of species
τ_s : characteristic time of species

Quasi-steady-state assumption (QSSA)

- If constant quasi-creation and destruction rates assumed, an analytical solution and the discretization form is derived

$$\boxed{Y_s^* = Y_s^m + \frac{\Delta t^*}{1 + \alpha_s^m p_s^m \Delta t^*}\left(q_s^m - p_s^m Y_s^m\right)}$$

where $\alpha_s^m = \frac{1 - \left(1 - e^{-p_s^m \Delta t^*}\right)/\left(p_s^m \Delta t^*\right)}{1 - e^{-p_s^m \Delta t^*}}$

⟶ The form is almost unconditionally stable

- Deviation of mass conservation due to the QSSA

$$\begin{aligned} \sum_s^N Y_s^* &= \sum_s^N Y_s^m + \sum_s^N \frac{\Delta t^*}{1 + \alpha_s^m p_s^m \Delta t^*}\left(q_s^m - p_s^m Y_s^m\right) \\ &= 1 + \boxed{\sum_s^N \frac{\Delta t^*}{1 + \alpha_s^m p_s^m \Delta t^*}\dot{\omega}_s^m} \neq 1 \end{aligned}$$

ERENA

Maintaining mass conservation property

- An optimized problem formulated by the Lagrange multiplier method

$$\boxed{\sum_{i=1}^{N}\frac{(y_i^{n+1}-y_i^*)^2}{2y_i^*}+\lambda\left(\sum_{i=1}^{N}y_i^{n+1}-1\right)=\epsilon}$$

y_i^* : Predictor values from integration methods

λ : Lagrange multiplier

ϵ : Auxiliary function

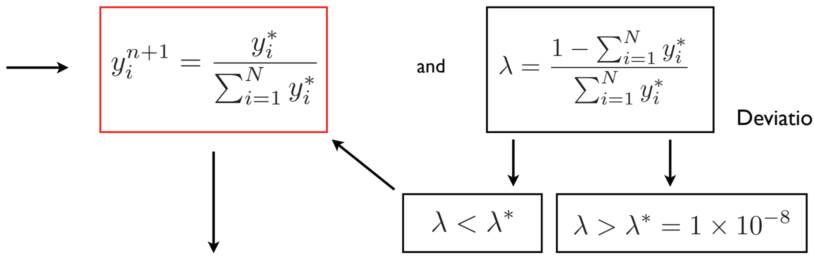

$$\longrightarrow \boxed{y_i^{n+1}=\frac{y_i^*}{\sum_{i=1}^{N}y_i^*}} \quad \text{and} \quad \boxed{\lambda=\frac{1-\sum_{i=1}^{N}y_i^*}{\sum_{i=1}^{N}y_i^*}}$$

Deviation error of mass conservation

$$\boxed{\lambda<\lambda^*} \qquad \boxed{\lambda>\lambda^*=1\times10^{-8}}$$

User specified

To the next step

Recomputing y_i^* with smaller time step sizes so that the mass conservation is satisfied

- Possible instability caused by the deviation of mass conservation can be eliminated
- Simple formulation — Program written in approximately 50 lines

Validation of ERENA

- Validated by experimental data and VODE solutions
- Significant performance (robustness and comp. time) compared to an implicit ODE and explicit solvers

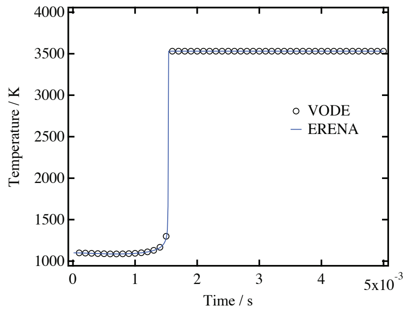

n-C_7H_{16}/O_2, 1 atm, 1100 K, Δt = 1.e-7 s

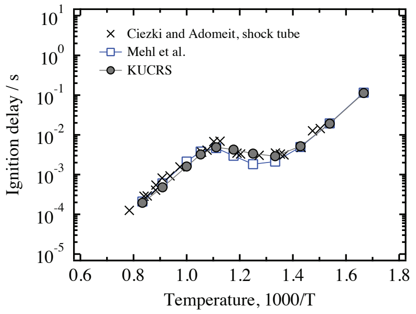

Comparison of ignition delay times with an experiment in case of n-heptane/air mixtures

340 times faster for n-C_7H_{16}

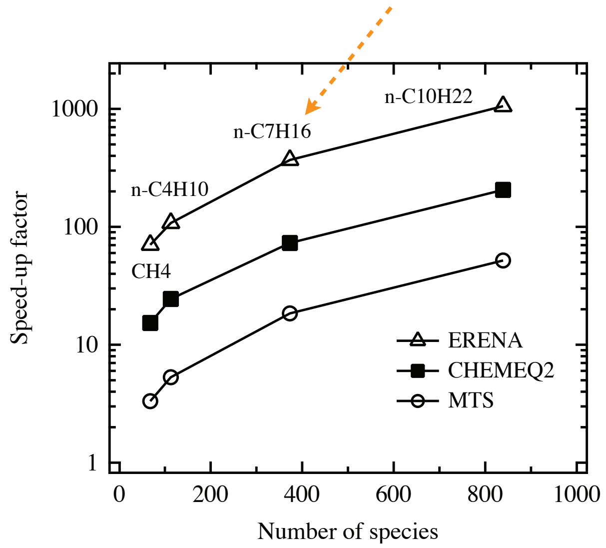

Comparison of computational time ERENA and other methods on several 0-D ignition problems with pure oxygen (the time step size of 1.e-8 s)

東京大学-JAXA社会連携講座シンポジウム，2018.01.22

CPU time histories

- Time history of CPU time per iteration to see superior performance of ERENA

CH_4/O_2, 1 atm, 1300 K, Δt = 1.e-8 s

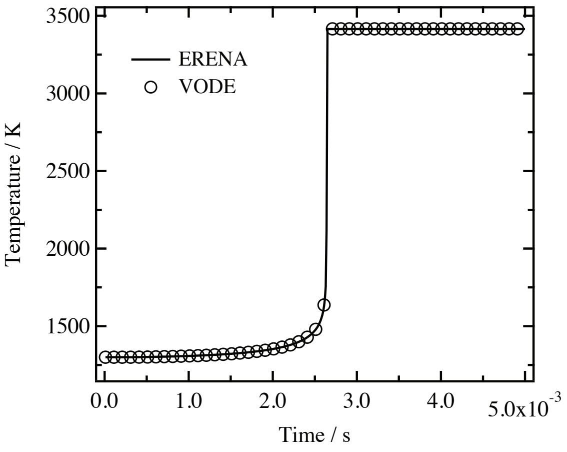

Temperature history

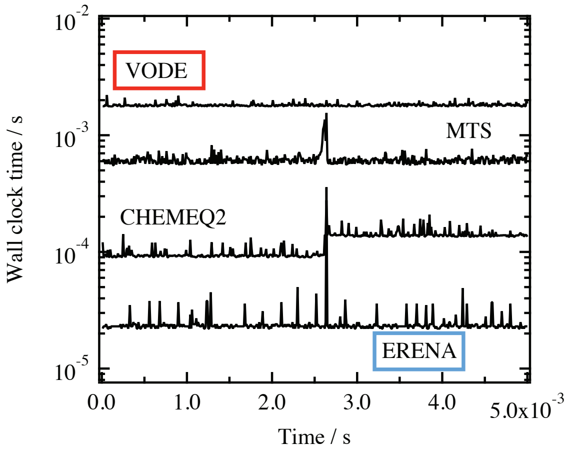

CPU time history

東京大学-JAXA社会連携講座シンポジウム，2018.01.22

Transport properties

- Occupancy of CPU times of each computational part

$$\frac{\partial(\rho Y_s)}{\partial t} + \nabla\cdot(\rho Y_s \boldsymbol{u} - \rho D_s \nabla Y_s) = \dot{\omega}_s$$

Species#
Transport properties

Stiffness

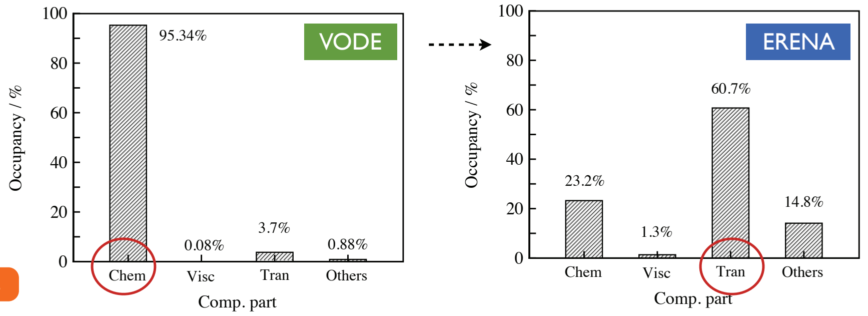

- **Species bundling technique** for diffusion coefficients

(Lu and Law, CNF2007)

- $n\text{-}C_7H_{16}$: 373 species bundled to 21 groups
- $n\text{-}C_4H_{10}$: 113 species bundled to 19 groups

57 times faster with 21 groups in $n\text{-}C_7H_{16}$

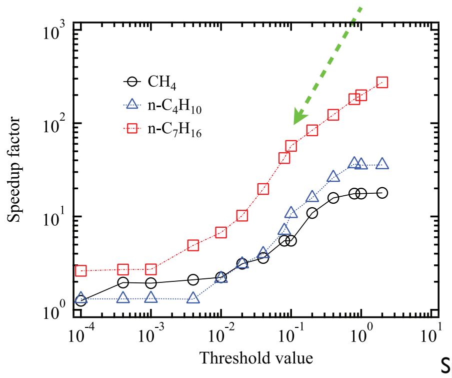

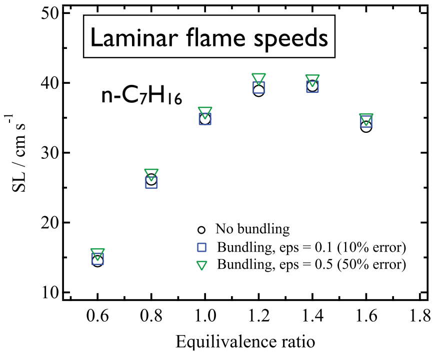

Speedup factor as a function of threshold values

Terashima et al., CNF2015, 2017

Internal combustion engine: knocking simulations

- ERENA/Species-bundling applied

- n-C_7H_{16} **(373 species, 1071 reactions)** and n-C_4H_{10} (113 species, 426 reactions) reaction mechanisms are directly considered (Terashima et al., CNF 2015, 2017)

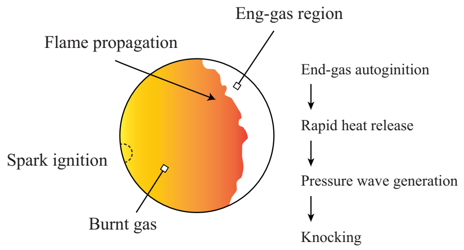

Schematic of a knocking combustion problem

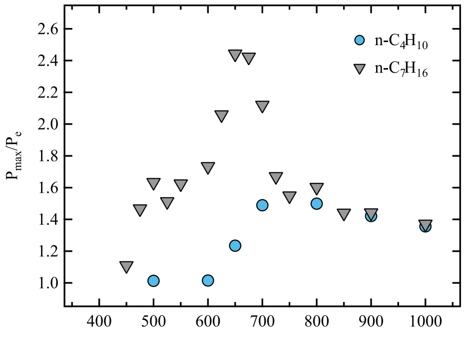

Knocking intensity

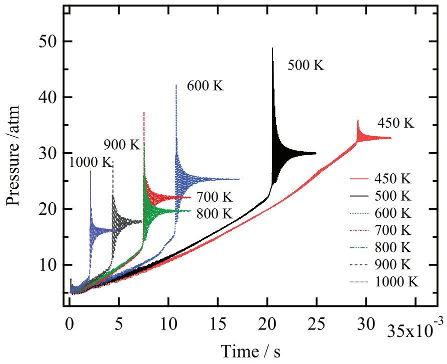

Pressure histories at the wall with the effects of temperatures

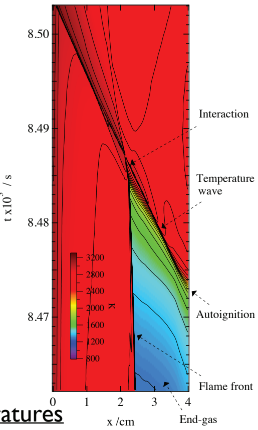

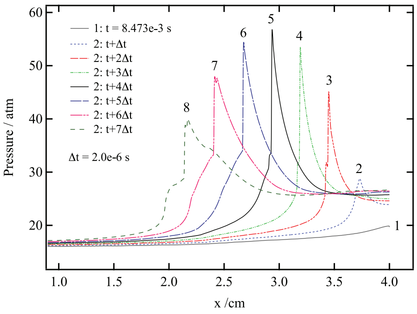

Development of pressure waves

Rocket combustion

1. Kendrick et al, CNF, 1999.
2. Candel et al., CST, 2006
3. Lux and Haidn, AIAA JPP 2009.

- Effects of recessed length on combustion flow fields of rocket-typed injectors [1-3]

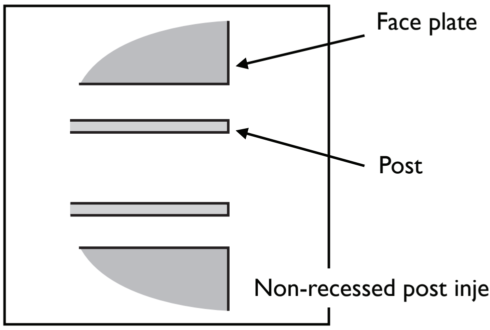

Non-recessed post injector

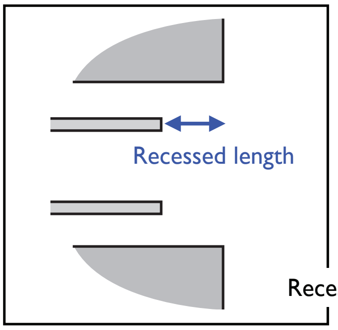

Recessed post injector

Recessed

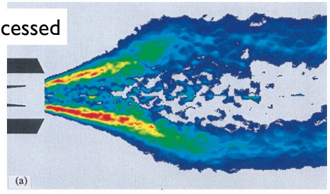

Non-recessed

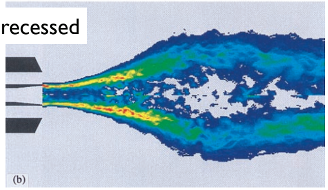

- Limitation of optical access into recessed regions

	mm
GOX internal diameter, d_1	4
GCH_4 internal diameter, d_2	5
GCH_4 external diameter, d_3	6
GOX post wall thickness	0.5
Recessed length	0, 3, 6, 9, 12
Domain hight, H	12
Domain length, L	250

referred as R0, R3, R6, R9, R12

Results: unsteady behaviors

- Near-injector flow fields with R9 case

Temperature

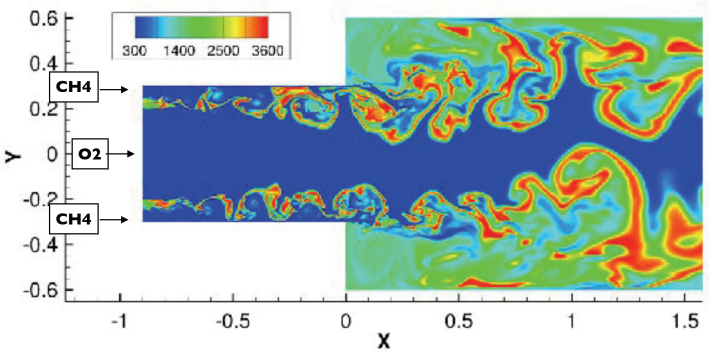

Mass fraction of CH_4

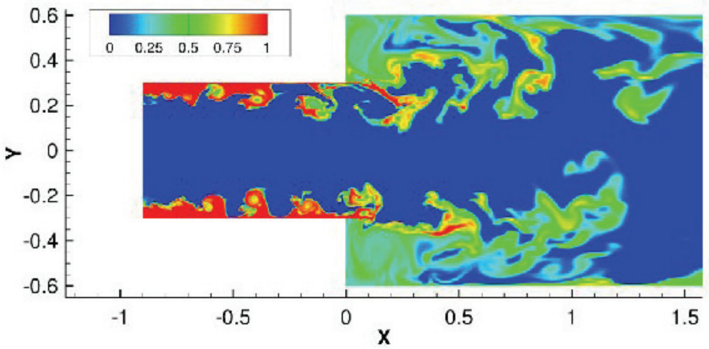

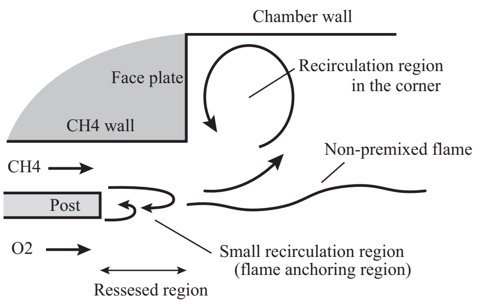

Schematic of combustion flow fields

No recessed case

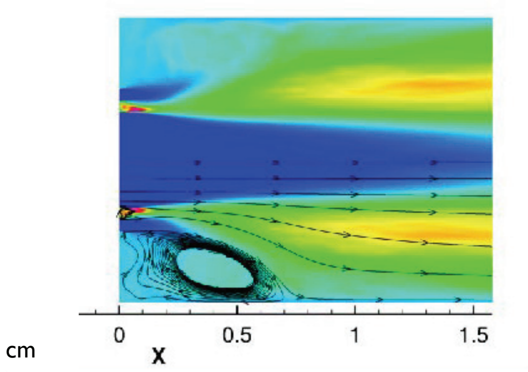

Mean temperature fields

- Effects of recessed length on mean combustion flow fields
- 1600 K contour for flame shape

R3

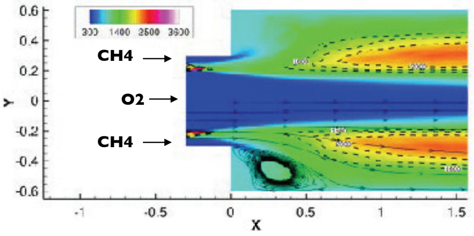

R6

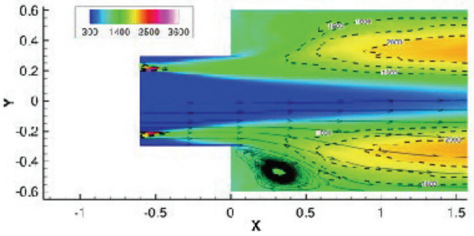

R9

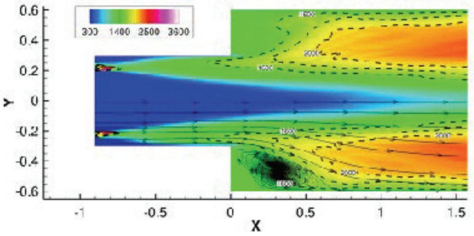

Increasing the recess length,

① larger amount of combustion gas produced in the recessed region

② larger flame angle in the chamber

③ higher temperature in the corner

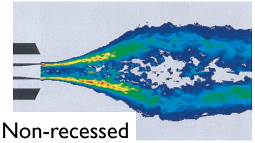
Non-recessed

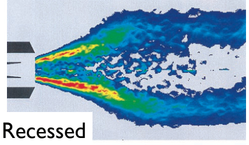
Recessed

R12 shows a different trend

R12

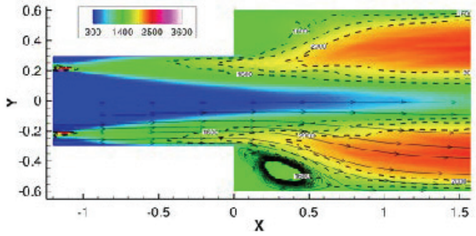

Mean temperature fields

R3

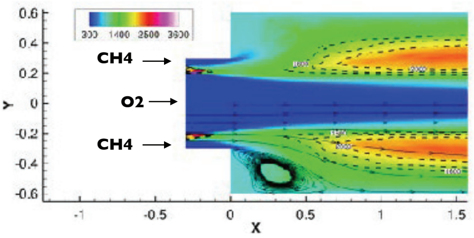

R6

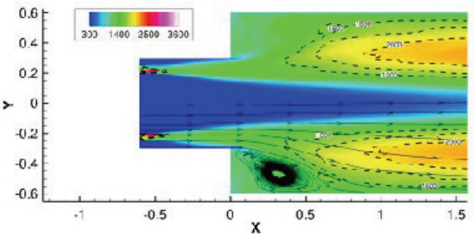

R9

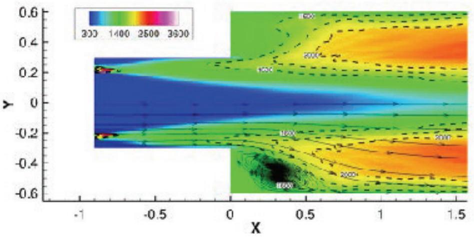

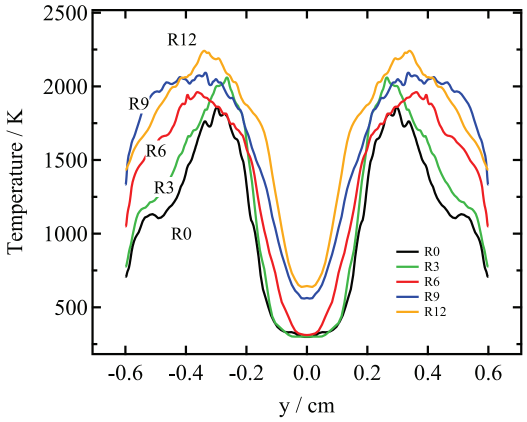

Mean temperature profiles at x = 0.75 cm

R12

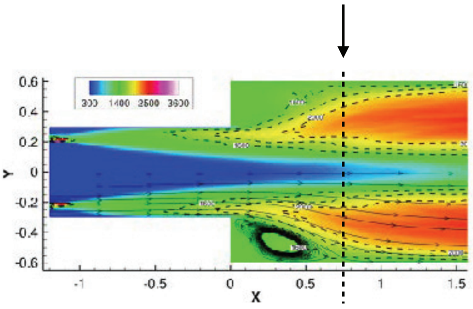

Mean velocity distributions

R3

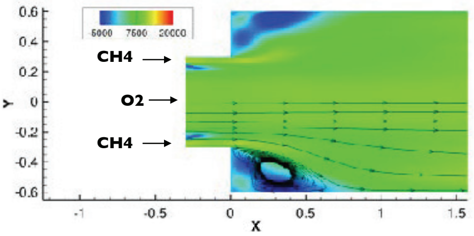

R6

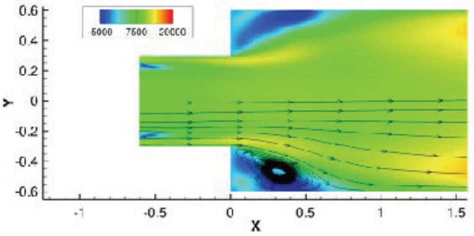

Increasing the recess length,

① larger amount of combustion gas produced in the recessed region

② combustion gas accelerated and higher x-velocity field generated

- Reducing a flame angle in the chamber with longer recessed cases

R9

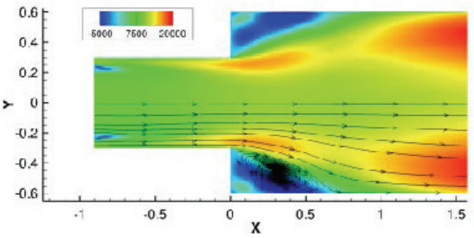

R12

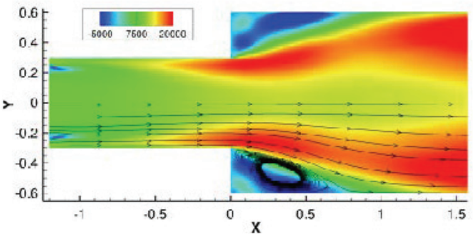

東京大学-JAXA社会連携講座シンポジウム，2018.01.22

Temperature in the recirculation region

R3

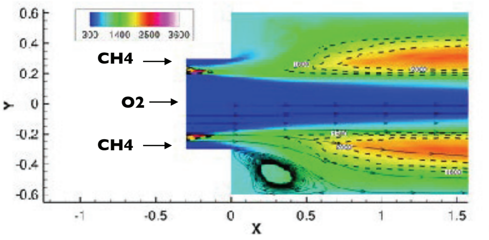

R6

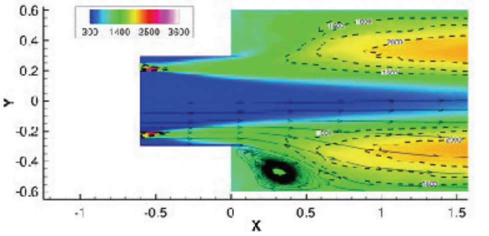

R9

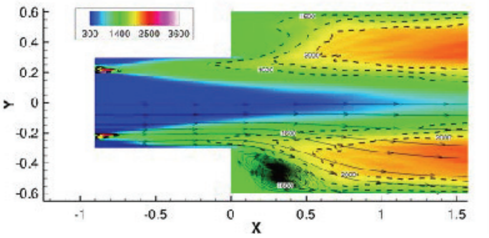

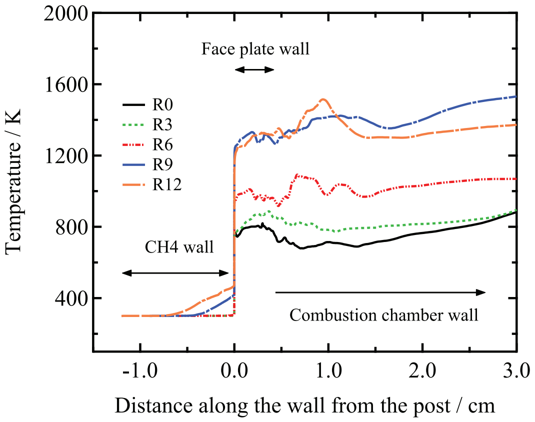

Mean temperature distributions in a coordinate along the wall

R12

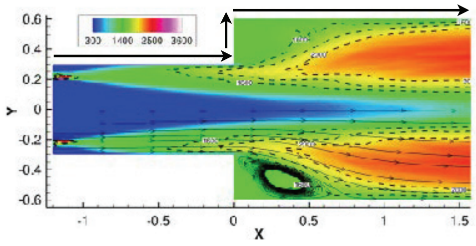

東京大学-JAXA社会連携講座シンポジウム，2018.01.22

Performance predicted

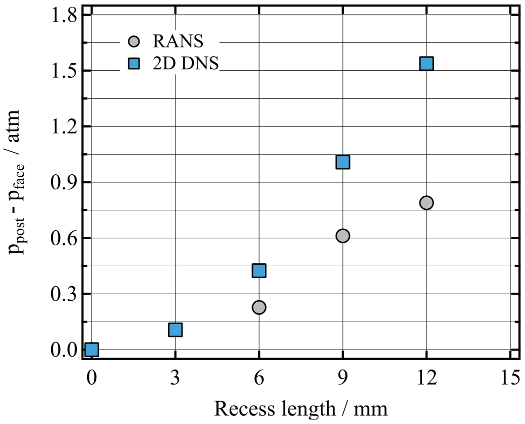

Pressure difference between the post and face plate

- Larger pressure differences in the recessed region with increasing recessed lengths

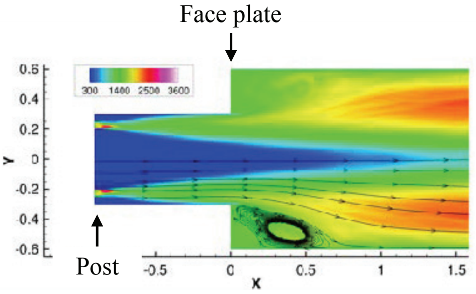

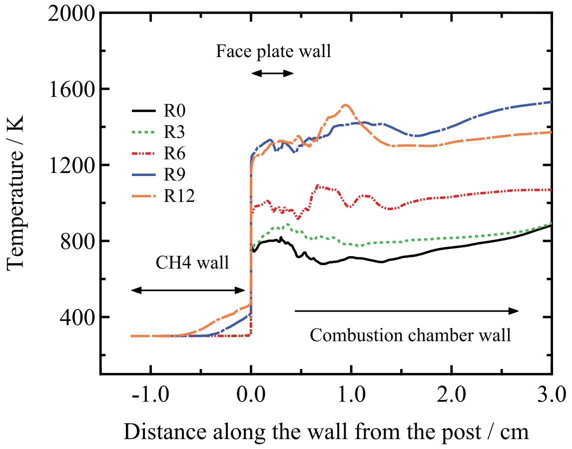

- R12 may have higher performance than R9; larger pressure loss and similar heat loss

Conclusions

- An efficient method for reactive flow simulations with large detailed chemistry has been originally developed under the collaboration between the University of Tokyo and JAXA
  - ERENA for time integration method of chemical reaction equations and species bundling technique for transport property calculations

- The present method has been successfully applied to various combustion problems
  - Tani et al., PCI2014 for hypergolic fuel combustion in spacecraft thruster
  - Terashima and Koshi, CNF2015 for knocking simulations of n-C7H16 and n-C4H10
  - Morii et al, JLPPI2015 for high-pressure hydrogen spontaneous ignition
  - Daimon et al., AIAA2016 for 3-D N2H4/NTO combustion flows
  - Matsugi and Terashima, CNF2017 for flame instability
  - Terashima et al., CNF2017 for hot-spot in knocking combustion
  - Tani et al., CST2018 for hypergolic spray combustion in spacecraft thruster